KJA
Korean Journal of Anesthesiology

Letter to the Editor

Korean J Anesthesiol 2022;75(3):286-289
https://doi.org/10.4097/kja.21290
pISSN 2005-6419 • eISSN 2005-7563

Received: June 29, 2021
Accepted: July 14, 2021

Corresponding author:
Nadia Hernandez, M.D.
Department of Anesthesiology and Perioperative Medicine, McGovern School of Medicine at UT Health, 6431 Fannin Street, MSB 5.020, Houston, TX 77030, USA
Tel: +1-832-289-5882
Fax: +7135006000
Email: nadia.hernandez@uth.tmc.edu
ORCID: https://orcid.org/0000-0002-7167-0461

The novel use of biplane imaging for ultrasound-guided regional anesthesia

Nadia Hernandez[1], Sudipta Sen[1], Johanna Blair de Haan[1], Stephen Haskins[2], Amit Pawa[3]

[1]Department of Anesthesiology and Perioperative Medicine, McGovern School of Medicine at UT Health, Houston, TX, [2]Department of Anesthesiology, Hospital for Special Surgery, Critical Care and Pain Management, New York, NY, USA, [3]Guy's & St Thomas' NHS Foundation Trust, London, UK

Ultrasound-guided regional anesthesia (USGRA) is commonly performed with B-mode (2D) imaging using high-frequency linear array and low-frequency curved array transducers. With biplane imaging (BI), phased array and high-frequency curved array (endocavity) transducers are available to evaluate cardiac and fetal anatomy and for needle guidance during transrectal procedures. BI capabilities have recently been incorporated into high-frequency linear transducers, making BI technology available for USGRA. During a peripheral nerve block (PNB), real-time BI eliminates the need to rotate the transducer to obtain both short-and long-axis views of the nerves, vessels, bones, muscles, or fascial planes. In addition, the needle is displayed in-plane and out-of-plane, and the spread of the local anesthetic can be visualized in two orthogonal planes simultaneously. Using BI for USGRA can decrease procedure time and the number of attempts and needle passes, improve block success and quality, and maximize safety by mitigating the risk of unintended intraneural, intrapleural, and intravascular injection. We report the novel use of BI for USGRA of the thorax, abdomen, and upper and lower extremities.

This technical report was exempt from internal review board approval since patient identifiable information were removed per institutional policies at the University of Texas Health Science Center at Houston and Memorial Hermann Hospital System, USA. Deidentified images were obtained from a regional anesthesia image bank. The highest quality images from each major region of the body were selected. Upper extremity biplane USGRA images, which are shown in Figs. 1A–1C, include interscalene, infraclavicular, and axillary brachial plexus blocks. Images of truncal fascial plane blocks are presented in Figs. 1D–1F, which include the superficial parasternal block, deep serratus plane block, and rectus sheath block. Figs. 1G and 1H highlight the high thoracic paravertebral block and the low thoracic erector spinae plane block. Finally, lower extremity biplane USGRA images of the femoral nerve block, distal femoral triangle block and popliteal sciatic nerve block are depicted in Figs. 1I–1K.

The Butterfly IQ+ (Butterfly Network, Inc., USA) ultrasound attached to either an iPhone 11 (iPhone 11 Pro-Butterfly iQ app) or a fifth generation iPad mini (iPad Butterfly iQ app) was utilized to perform biplane USGRA. The standard B-mode image (reference plane) is displayed at the bottom of the screen, while the orthogonal plane that correlates to the curser (perpendicular plane) is shown at the top of the screen. The transducer was positioned to be simultaneously perpendicular to the object of interest in the short axis and parallel in the long axis to ensure optimal BI. A 20–22 gauge blunt-tip 50–100 mm echogenic block needle (B Braun Ultraplex 360, USA) or 18-gauge SonoTAP Tuohy needle (PAJUNK GmbH Medizintechnologie, Germany) was advanced to the target location for each block using the reference plane and an in-plane technique. The biplane cursor

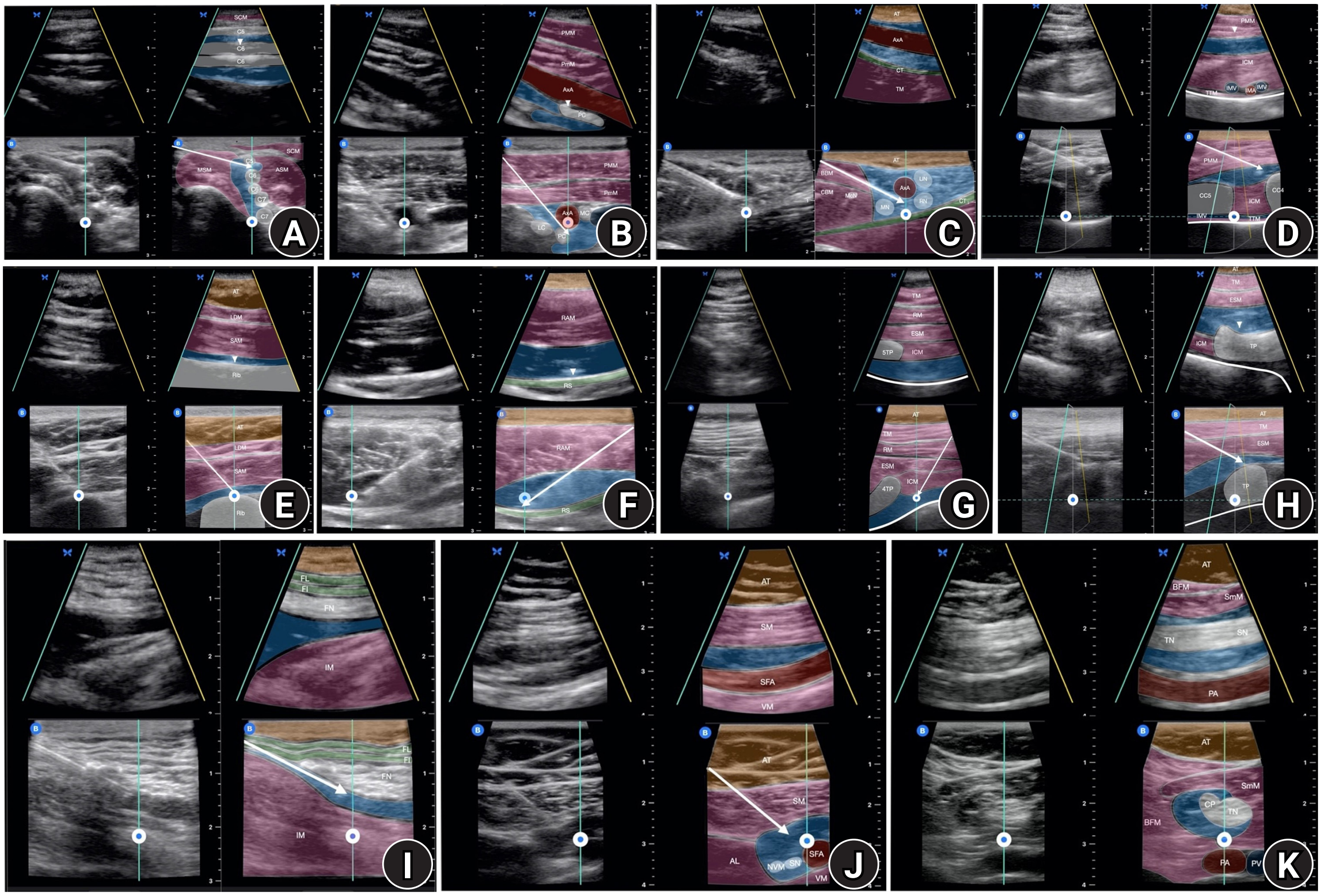

Fig. 1. (A) Interscalene brachial plexus block. The ultrasound was placed over the clavicle in a transverse orientation. In the reference plane, the orientation marker (OM) is lateral, and the brachial plexus, ASM, MSM, VA, and the SCM are displayed in the short-axis view, while the seventh cervical transverse process is seen in the long-axis view. The needle trajectory is in-plane lateral to medial. The biplane cursor is over the C5 and C6 nerve roots. In the perpendicular plane, the icon is caudal. The needle trajectory is out-of-plane, and the tip can be seen between C5 & C6 in long-axis. The craniocaudal spread of the local anesthetic (LA) within the brachial plexus is visualized. In all images, the white arrow represents the needle shaft on the ultrasound and the white arrowhead represents the needle tip on the ultrasound. (B) Infraclavicular brachial plexus block. The ultrasound was placed over the lateral chest in a sagittal orientation. In the reference plane, the OM is cranial with the brachial plexus and AxA are displayed in short-axis. The needle trajectory is in-plane with the biplane cursor directly over the AxA. In the perpendicular plane, the icon is lateral. The needle trajectory is out-of-plane. The AxA and the mediolateral spread of LA are visualized in long-axis. (C) Axillary brachial plexus block. The ultrasound was placed over the axilla in a sagittal orientation. In the reference plane, the OM is superior, and the branches of the brachial plexus, AxA, and vein are displayed in short-axis. The needle trajectory is in-plane in the superior- inferior direction. The needle reverberation artifact makes it challenging to identify the MN and McN in this image. The biplane cursor is located directly over the AxA. In the perpendicular plane, the icon is lateral. The needle trajectory is out-of-plane. The AxA and mediolateral spread of the LA within the brachial plexus are visualized in long-axis. The needle is not seen on the long axis view in this image as the biplane sector is distal to the needle tip. (D) Superficial parasternal block. The ultrasound transducer is placed over CC4 in a sagittal orientation. In the reference plane, the OM is caudal, CC4 and CC5 are displayed in short-axis, while the IMV is seen in long-axis. The needle trajectory is in-plane in the craniocaudal direction. The biplane cursor is directly over the fourth intercostal space. In the perpendicular plane, the icon is lateral. The needle trajectory is out-of-plane, and the shaft of the needle can be seen traversing the PMM. The internal mammary vessels and the mediolateral spread of LA between the PMM and ICM are seen in short-axis. (E) Deep serratus plane block. The ultrasound was placed over the posterior axillary line in a sagittal orientation. In the reference plane, the OM is cranial, and the fifth rib is displayed in short-axis. The needle trajectory is in-plane. The biplane cursor is directly over the fifth rib. In the perpendicular plane, the icon is anterior. The needle trajectory is out-of-plane with the needle tip visible deep to the SAM. The fifth rib and the anteroposterior spread of the LA are visualized in long-axis. (F) Rectus sheath block. The ultrasound was placed over the mid-abdomen in a sagittal orientation. In the reference plane, the OM is medial, and the RAM is displayed in short-axis. The needle trajectory is in-plane. The biplane cursor is placed directly over the tip of the needle. In the perpendicular plane, the icon is cranial. The craniocaudal spread of the LA and the tip of the needle are visualized in short-axis. The white arrow represents the needle on the ultrasound. The white arrowhead represents the needle tip on the ultrasound. (G) Thoracic paravertebral block. The ultrasound was placed over the 4TP in a transverse orientation. In the reference plane, the OM is medial, and the 4TP is displayed in long-axis. The needle trajectory is in-plane. The biplane cursor is directly over the paravertebral space. In the perpendicular plane, the icon is caudal. 5TP and the craniocaudal spread of the LA are visualized in short-axis.

The white arrow represents the needle on the ultrasound. (H) Erector spinae plane block. The ultrasound was placed over the tenth TP in a sagittal orientation at an approximately 20-degree clockwise rotation. In the reference plane, the OM is caudal, and the TP is displayed in short-axis. The needle trajectory is in-plane. The biplane cursor is directly over the TP. In the perpendicular plane, the icon is lateral. The TP and the mediolateral spread of the local anesthetic are visualized in long-axis. The white arrow represents the needle on the ultrasound. The white arrowhead represents the needle tip on the ultrasound. (I) Femoral nerve block. The ultrasound is placed over the inguinal ligament in a transverse orientation to identify the femoral nerve, artery, and vein. In the reference plane, the OM is lateral, and the FN is displayed in short-axis. The needle can be visualized in-plane. The mediolateral spread of the LA is noted in this plane. The biplane cursor is located over the FN. In the perpendicular plane, the icon is cranial. The FN and craniocaudal spread of the LA are visualized in the long-axis view. The white arrow represents the needle on the ultrasound. (J) Distal femoral triangle block. The ultrasound was placed over the medial thigh in a transverse orientation. In the reference plane, the OM is medial, and the SFA, SN, and NVM are displayed in short-axis. The circumferential spread of the LA around the SFA is noted in this plane. The biplane cursor is located over the SFA. The icon is inferior in the perpendicular plane. The SFA and craniocaudal spread of the LA are visualized in long-axis. (K) Popliteal sciatic nerve block. The ultrasound was placed over the bifurcation of the SN into TN and CP nerve in a transverse orientation. In the reference plane, the OM is lateral, and the TN and CP nerve are displayed in short-axis after a popliteal sciatic block. The circumferential spread of the local anesthetic is visualized in this plane. The biplane cursor is located over the TN and PA. The icon is inferior in the perpendicular plane. Superiorly, the SN is visualized in long-axis. Inferiorly, the TN, PA and craniocaudal spread of the local anesthetic are visualized in long-axis. SCM: sternocleidomastoid muscle, ASM: anterior scalene muscle, MSM: middle scalene muscle, C: vertebral artery, C5: fifth cervical nerve root, C6: sixth cervical nerve root, C7: seventh cervical nerve root, PMM: pectoralis major muscle, PmM: pectoralis minor muscle, AxA: axillary artery, PC: posterior cord, AxV: axillary vein, MC: medial cord, LC: lateral cord, AT: adipose tissue, CT: conjoint tendon, TM: triceps muscle (C), BBM: biceps brachii muscle, CBM: coracobrachialis muscle, McN: musculocutaneous nerve, MN: medial nerve, RN: radial nerve, UN: ulnar nerve, ICM: intercostal muscles, IMV: internal mammary vein, IMA: internal mammary artery, CC5: fifth costal cartilage, CC4: fourth costal cartilage, TTM: transverse thoracic muscle, LDM: latissimus dorsi muscle, SAM: serratus anterior muscle, RAM: rectus abdominis muscle, RS: rectus sheath, TM: trapezius muscle (G&H), RM: rhomboid muscle, ESM: erector spinae muscle, 5TP: fifth transverse process, 4TP: fourth transverse process, TP: transverse process, FL: fascia lata, FI: fascia iliaca, FN: femoral nerve, IM: iliacus muscle, SM: sartorius muscle, SFA: superficial femoral artery, VM: vastus medialis muscle, AL: adductor longus muscle, NVM: nerve to vastus medialis, SN: saphenous nerve (J), BFM: biceps femoris muscle, SmM: semimembranosus muscle, SN: sciatic nerve (K), TN: tibial nerve, PA: popliteal artery, CP: common peroneal nerve, PV: popliteal vein.

was placed over the needle tip for visualization in the short-axis view, on the neurovascular structures to obtain images of the entire nerve or artery in the long-axis view, and/or bone, muscle, or fascial planes of interest to obtain an orthogonal view. The biplanar spread of the local anesthetic was observed upon injection.

BI can be activated at any time; however, due to the reduced screen size and image quality, we recommend timing it on a case-by-case basis. For superficial blocks, where needle visualization is less challenging, BI can be activated when the optimal monoplane image is obtained in B-mode. For deeper blocks, where needle localization is more difficult to confirm sonographically, we recommend advancing the needle in B-mode and activating BI once the needle tip is in the desired location to improve the accuracy and visualization of the local anesthetic injectate as it spreads orthogonally through the tissue planes.

The use of BI for superficial ultrasound-guided (USG) vascular access has been reported using low- and high-frequency matrix transducers. One study concluded that the enhanced visualization of structures and needles leads to improved performance and feasibility. For internal jugular vein (IJV) cannulation using the short-axis approach, applying BI with a low-frequency matrix transducer resulted in fewer puncture attempts and needle redirections, a lower incidence of posterior wall punctures, and successful puncture of the IJV on the first attempt in 90% of cases vs. 50% with B-mode [1]. The low-frequency transducer used in this study, which is designed for imaging large, superficial vascular structures, is acceptable for IJV cannulation; however, it provides suboptimal visualization of small superficial structures, such as nerve roots for USGRA [2]. For the case presented by Convissar et al. [3], a semiconductor-based ultrasound with a high-frequency setting (vascular) was used to perform radial artery cannulation with BI. To date, this case is the only report of BI needle-guidance for high-frequency ultrasound. The use of BI for USGRA has not previously been reported. Therefore, in this study, we included images of the USG PNB and fascial plane blocks using the novel application of a high-frequency ultrasound transducer (Figs. 1A–1K).

The spread of injectate following the PNB was studied through cadaveric dissection after dye or radiologic contrast injections. However, this type of study has been criticized since postmortem alterations in tissue integrity could affect the patterns of injectate spread and may not accurately represent clinical situations. In the clinical setting, arterial pulsations, muscle contractions, respirations, and differences in tissue resistance can influence the spread of local anesthetics [4]. Although BI technology is not currently available in the most common ultrasound systems used for USGRA, enhanced imaging may improve our understanding of sonoanatomy and the spread of local anesthesia. In 2019, a high-frequency matrix linear array piezoelectric transducer was introduced into the market for vascular applications (Philips XL

https://doi.org/10.4097/kja.21290

14-3 mMatrix, Netherlands). In 2020, BI for a high-frequency handheld ultrasound became commercially available (Butterfly Network, Inc., USA). Rapid technological advances in ultrasound coupled with the potential for enhanced superficial imaging might lead to a future where matrix 3- and 4-dimensional imaging for USGRA is the standard.

BI is a new feature in high-frequency matrix ultrasound transducers that can improve needle localization and enhance visualization of local anesthetic spread during USGRA. We reported on the novel application of BI for USGRA. More studies are needed to assess the utility of BI in USGRA and evaluate its impact on the safety and delivery of regional anesthesia.

Funding

None.

Conflicts of Interest

No potential conflict of interest relevant to this article was reported. Nadia Hernandez and Amit Pawa have received honoraria from Butterfly Network, Inc. for educational activities unrelated to this article.

Author Contributions

Nadia Hernandez (Conceptualization; Visualization; Writing – original draft; Writing – review & editing)
Sudipta Sen (Writing – review & editing)
Johanna Blair de Haan (Writing – original draft; Writing – review & editing)
Stephen Haskins (Writing – original draft; Writing – review & editing)
Amit Pawa (Conceptualization; Visualization; Writing – original draft; Writing – review & editing)

ORCID

Nadia Hernandez, https://orcid.org/0000-0002-7167-0461
Sudipta Sen, https://orcid.org/0000-0001-6159-1092
Johanna Blair de Haan, https://orcid.org/0000-0002-6976-2041
Stephen Haskins, https://orcid.org/0000-0001-8012-7594
Amit Pawa, https://orcid.org/0000-0002-2404-9162

References

1. Panidapu N, Babu S, Koshy T, Sukesan S, Dash PK, Panicker VT. Internal jugular vein cannulation using a 3-dimensional ultrasound probe in patients undergoing cardiac surgery: comparison between biplane view and short-axis view. J Cardiothorac Vasc Anesth 2021; 35: 91-7.
2. Huang J, Li J, Wang H. The principles and procedures of ultrasound-guided anesthesia techniques. Cureus 2018; 10: e2980.
3. Convissar D, Bittner EA, Chang MG. Biplane imaging using portable ultrasound devices for vascular access. Cureus 2021; 13: e12561.
4. Daga V, Narayanan MK, Dedhia JD, Gaur P, Crick H, Gaur A. Cadaveric feasibility study on the use of ultrasound contrast to assess spread of injectate in the serratus anterior muscle plane. Saudi J Anaesth 2016; 10: 198-201.